Chapter 5

Results and Discussions

In this chapter, we describe the experimental results and discussions for the deposition and the properties of Ga-doped ZnO thin films fabricated in this thesis work. The dependence of the depostion rate and the structural properties of the films on the sputtering conditions will be shown. The electrical and optical properties of GZO thin films are shown that they depend on Ga_2O_3 contents in the target and the conditions of the deposition process.

5.1 Deposition Rate of the GZO Thin Films

Figure 5.1 shows the dependence of the deposition rate versus the RF power used in the sputtering process. For a given argon (Ar) gas pressure, the deposition rate is found to be proportional to the RF power. The deposition rate, which is the average value of each position of a sample, increases as the RF power increases. It can be explained that the ionization of Ar gas atoms increases when the RF power increases. The positive gas ions increase and have higher energy due to the increasing of both applied current and applied voltage. The GZO target is then bombarded by high energetic particles, resulting in more sputtered atoms and ions arriving the substrate. Therefore, at the same deposition time, the films deposited by high RF power will be thicker than those deposited by low RF power.

Figure 5.2 shows the dependence of the deposition rate on the sputtering Ar pressure (P_{Ar}). For the same RF power, the deposition rate decreases slightly as Ar

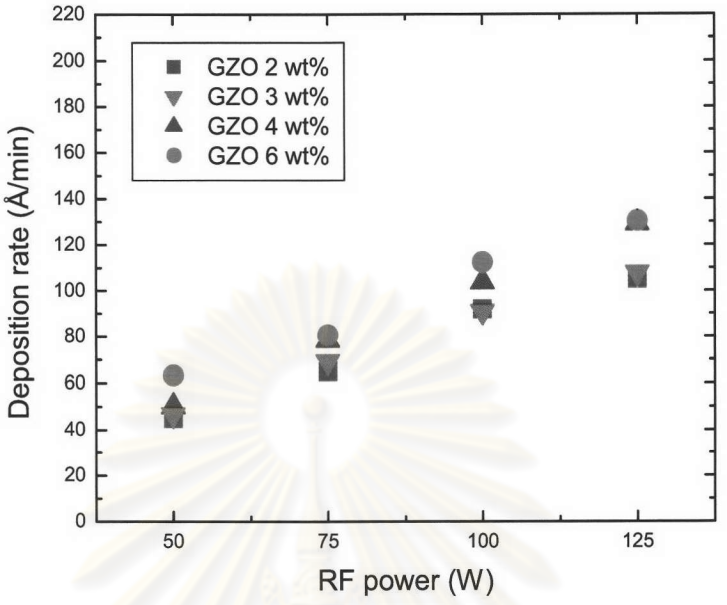

Figure 5.1: Dependence of the deposition rate on the sputtering RF power for the GZO thin films

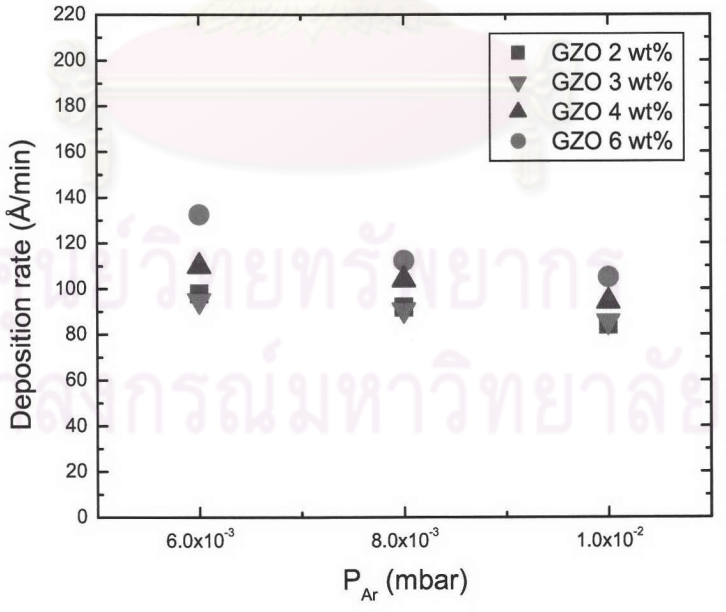

Figure 5.2: Dependence of the deposition rate on the sputtering Ar pressure for the GZO thin films

pressure increases. For higher Ar pressure, the mean free path of sputtered species in the chamber decreases and undergoes many collisions leading to the decreasing of kinetic energy. Therefore, the mobility of these species decreases and the deposition rate also decreases. However, consider a GZO target, the deposition rates in each Ar pressure conditions differ in narrow range. For example, the deposition rates of sputtering the target with 2 wt% Ga_2O_3 at varied Ar pressures were in the range $84 - 98$Å$/\min$. On the other hand, The deposition rates of sputtering the same target with increasing of RF power from 75 W to 100 W were around $65 - 92$Å$/\min$ range. The deposition rates as varying RF power were more significant than those with varying Ar pressure.

5.2 Structural Properties

Figure 5.3 shows the XRD patterns of GZO thin films deposited at a thickness of 3153, 7207 and 10995 Å, using Ar gas pressure of 8.0×10^{-3} mbar and RF power of 100 W. For such films, they were deposited by using the target with Ga_2O_3 content of 6 wt%. The XRD measurements were taken on the central region of the samples. The only (002) diffraction peak was observed at $2\theta \approx 34.1°$, revealing that all of the obtained films were polycrystalline with a hexagonal structure, and a preferred orientation with the c-axis perpendicular to the substrate. These peaks showed deviations from 34.44° which is the value of standard ZnO powder (JCPDS: 05-0664) but they were close to 34.2° of the non-doped ZnO thin film prepared at RF power of 150 W by Park *et al.* [33]. The intensity of the peak increases significantly when the film thickness increases from 3153Å to 7207Å. The increase in the peak height with increasing thickness reveals that increasing the thickness improves the crystallinity of the film. We note that for the films prepared using this sputtering condition, the intensity of the XRD peaks reaches the saturation when the film thickness is more than 7000Å.

The results in Figs. 5.4(a) - (c) suggest that the crystallinity of the film depends on the RF power. At the same Ga_2O_3 content, the peak intensity decreases

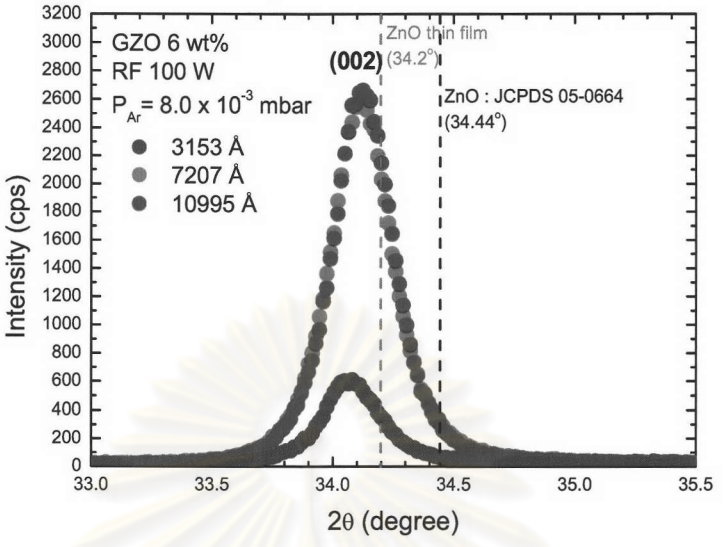

Figure 5.3: X-ray diffraction patterns for GZO thin films with different thicknesses deposited at RF power of 100 W and $P_{Ar} = 8.0 \times 10^{-3}$ mbar by using the target with Ga_2O_3 content of 6 wt%

with the increasing of the RF power. The sharp peaks observed for ZnO (002) plane indicate a strong c-axis orientation. It shows that lower sputtering power yields better crystallinity of the films, as can be seen from the intensities of the diffraction peaks were more intense and sharper when RF power was decreased.

As previously discussed, the deposition rate is proportional to the RF power. Consider the thin film formation [26], the crystal growth is encouraged by low deposition rate because the sputtered atoms also take time to find an energetically favourable lattice position. On the other hand, when the deposition rate increases, many sputtered atoms probably arrive the substrate while other atoms were diffusing on the surface of the deposited film. It suggests that the sputtered atoms could not be arranged into suitable lattice sites in the crystal structure of the films. Thus, the crystallinity can be improved by decreasing the deposition rate by lowing the RF power as shown in Figs. 5.4 and 5.5. The films shown in Fig. 5.5 were deposited at the RF power of 50 W and 100 W with the deposition time of 200 mins and 90

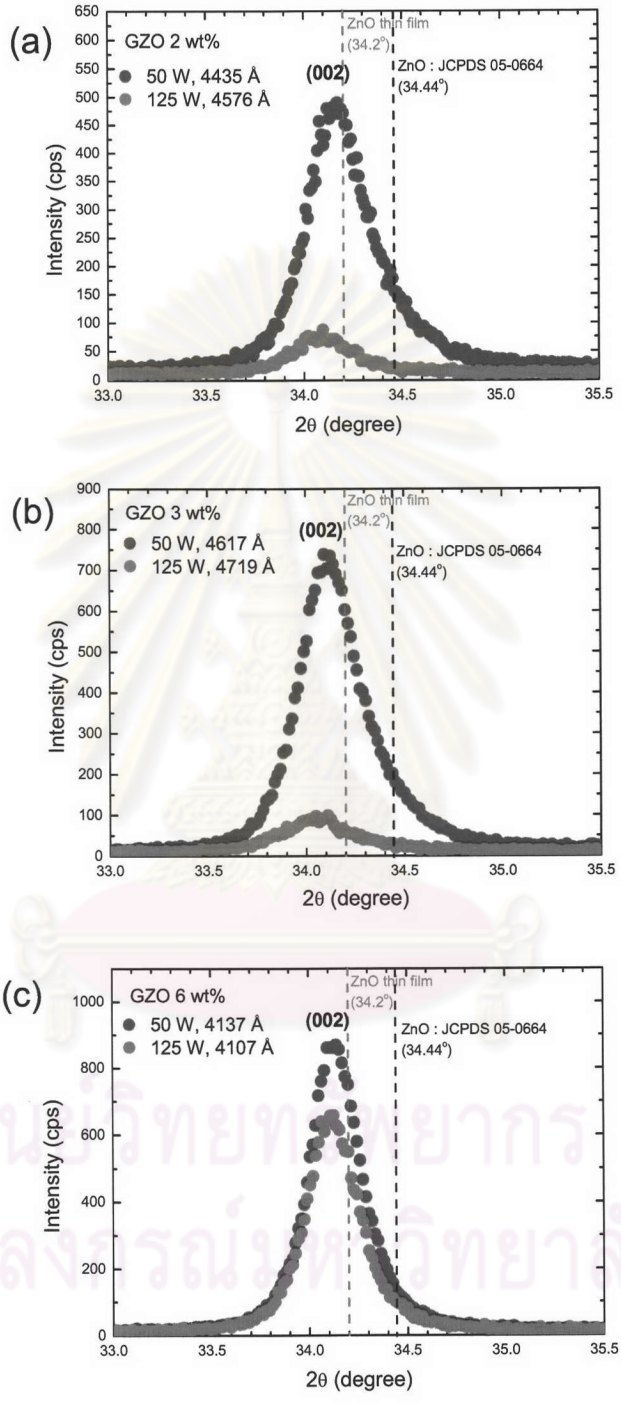

Figure 5.4: XRD patterns for GZO thin films prepared at RF power of 50 and 125 W using the the target with Ga_2O_3 content of 2, 3 and 6 wt% ((a) - (c)) at Ar pressure of 8.0×10^{-3} mbar

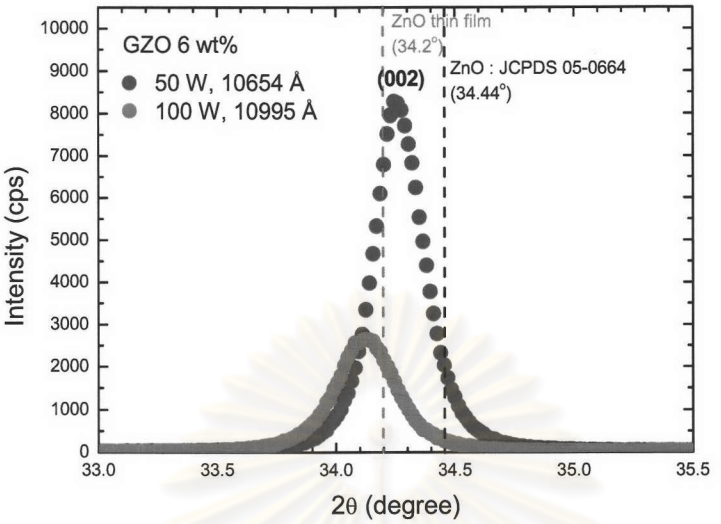

Figure 5.5: XRD patterns for GZO thin films at the same thickness prepared at RF power of 50 and 100 W using the the target with Ga_2O_3 content of 6 wt% at Ar pressure of 8.0×10^{-3} mbar

mins, respectively. The grain size D can be estimated using Scherrer formula [34]

$$D = \frac{0.94\lambda}{\beta \cos\theta}, \tag{5.1}$$

where λ is the wavelength of the X-rays (1.5405 Å), θ is the Bragg diffraction angle at the peak position in degree, and β is the full-width at half-maximum (FWHM) in radian. This gives the estimated grain size D of 33 nm and 39 nm at the RF power of 100 W and 50 W, respectively. It suggests that lower deposition rate leads to larger grain size and better crystallinity.

It can be expected that the deposition rate related to the RF power is an important factor forming non-stoichiometric or nearly stoichiometric of the composition ratio between the oxygen and zinc atomic in the films. Lin *et al.* [35] and Bachari *et al.* [31] studied ZnO thin films deposited by RF magnetron sputtering and reported that the films became non-stoichiometric at high RF power. The non-stoichiometric or oxygen deficiency leaded to the growth of less homogeneous films with more crystallographic faults, and a decrease in long range order in the sputtered films. It suggested that the non-stoichiometric films displayed poor crys-

tallinity [31, 35]. Thus, the GZO thin films prepared at high RF power are proposed to be non-stoichiometric. On the other hand, a near stoichiometric oxide can be formed with decreasing RF power.

In addition, every XRD pattern shows that the ZnO (002) peak is left shifted from 33.44° which is the value of standard ZnO powder. However, it is close to the peak of non-doped ZnO thin film [33], which is used to show that the thin films prepared by sputtering technique are suffering from stress. By following the Bragg law

$$\lambda = 2d \sin\theta, \tag{5.2}$$

where d is the interplanar spacing and θ is the diffraction angle. It can be explained that the decrease of the diffraction angle θ results in the increase of interplanar spacing since the λ is fixed. All the data show that all thin films have the d values higher than that of the ZnO powder. There is the strain occurring in the films. It indicates that all GZO thin films exhibited the stresses as well as the non-doped ZnO thin film. The film stress is caused by the imperfection of the crystal structure due to the deposition process [36, 37]. Figure 5.5 shows the XRD pattern for the GZO 6 wt% thin films deposited with the same thickness at the RF power of 50 and 100 W. The peak position is slightly changed from $2\theta = 34.26°$ to 34.12° with increasing RF power. This suggests that the film suffers more stress with the increase of the sputtering power related to the deposition rate.

These were confirmed by post deposition annealing of the samples in air atmosphere. The samples were annealed at 200°C and 400°C in air atmosphere for 2 hrs, as shown in Fig. 5.6. Figures 5.6(a) and (b) show the XRD patterns of GZO 2 wt% thin films deposited at power 100 W. The XRD patterns of GZO 4 wt% thin films deposited at power 50 and 125 W are shown in Figs. 5.6(c) and (d), respectively. These films were deposited under sputtering Ar pressure of 8.0×10^{-3} mbar.

Figure 5.6(a) shows a comparison of the XRD patterns of the samples before and after annealing at the temperature of 200°C for 2 hrs in air atmosphere. The

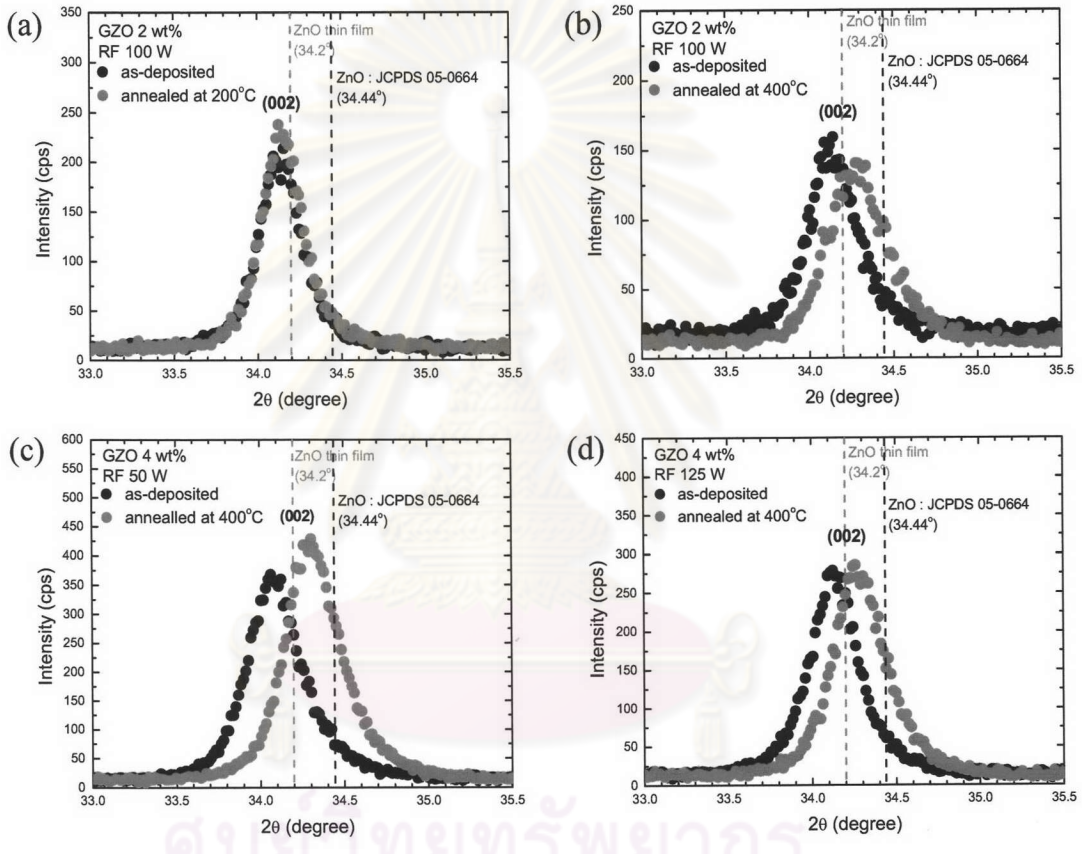

Figure 5.6: XRD patterns for GZO thin films deposited with various sputtering parameters before and after annealing in air atmosphere at 200°C and 400°C for 2 hrs

peak position did not show a shift after annealing. On the other hand, the peak position of GZO thin films shifted toward the higher angle with the increase of annealing temperature to 400°C, as can be seen in Figs. 5.6(b) - (d). The post deposition annealing at high temperature leads to a decrease of interplanar spacing d values that become closer to that of the standard powder. This suggests that annealing seems to provide energy for structural rearrangement, resulting in a relaxation of the films. However, it is not sufficient to improve the film crystallinity. This is supported by the data shown in Fig. 5.6 that the intensity of XRD spectra was not significantly changed. This means the crystallinity of the film does not change after the post deposition annealing in air atmosphere.

Furthermore, the annealing, which performed in air atmosphere, affected oxygen O_2 and nitrogen N_2 absorption of the film. The molecules of O_2 and N_2, which have higher kinetic energy, can be absorbed into the films. This behaviour is called chemisorption of O_2 and N_2 [32]. It affects to the electrical properties of the film which will be discussed in the next section.

5.3 Electrical Properties

In our set up, the substrates are rotated in circle parallel and off-axis to the surface of target during the planar sputtering. The deposited films show non-uniformity and can be divided into three zones, A, B and C, according to radius of the rotation as shown in Fig. 5.7.

The films were deposited at room temperature and the same Ar pressure of 8.0×10^{-3} mbar. In Fig. 5.8, we show the results of the resistivity of the films with Ga_2O_3 contents of 2wt% and 6wt%, in each zone of the substrate as we varied the RF power. The Hall measurement shows that the GZO thin films are degenerate doped n-type semiconductor.

It can be observed clearly for the GZO of 2wt% thin film that when the RF power increases from 50 W to 125 W, the resistivity of each zone decreases from

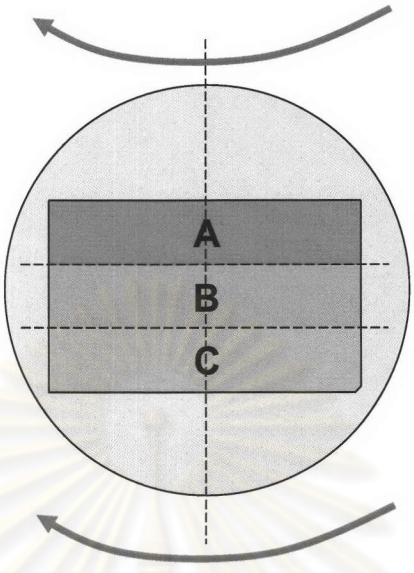

Figure 5.7: Three zones of deposited thin films according to radius of the substrate rotation

the order of 10^{-1} Ω·cm to the order of 10^{-3} Ω·cm. In the case of GZO 6wt%, the resistivity of the film in each zone differs insignificantly and is at about the same order as deposited by different RF power. Therefore, the trend of dependence of resistivity on the RF power can be observed only in the case of low Ga_2O_3 content.

The resistivity dependence on Ga_2O_3 content is shown in Fig. 5.9. The films were deposited at low and high RF power of 50 W and 125 W under Ar pressure of 8.0×10^{-3} mbar. It shows that the resistivity decreases with increasing Ga_2O_3 content and RF power. The resistivity of each zone of the films deposited at low RF power and low Ga_2O_3 content (2 and 3 wt%) differs significantly, but it is very close at high RF power in all Ga_2O_3 content as well as the case of deposition at high Ga_2O_3 content in all RF power. From Figs. 5.8 and 5.9, the GZO thin films with low resistivity in the range of 10^{-3}Ω·cm are more uniform. In addition, the resistivity of each zone is about the same which decreases when the Ga_2O_3 content increases. In our electrical measurement, we use only the central part of the substrate.

Figure 5.10 shows the dependence of the resistivity, the mobility and the carrier concentration versus Ga_2O_3 content. Both carrier concentration and mobility

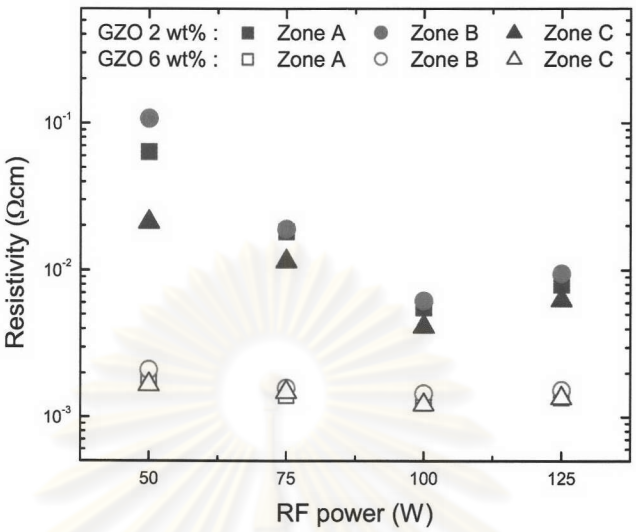

Figure 5.8: Resistivity of each zone of the GZO films versus the RF power at $P_{Ar} = 8.0 \times 10^{-3}$ mbar

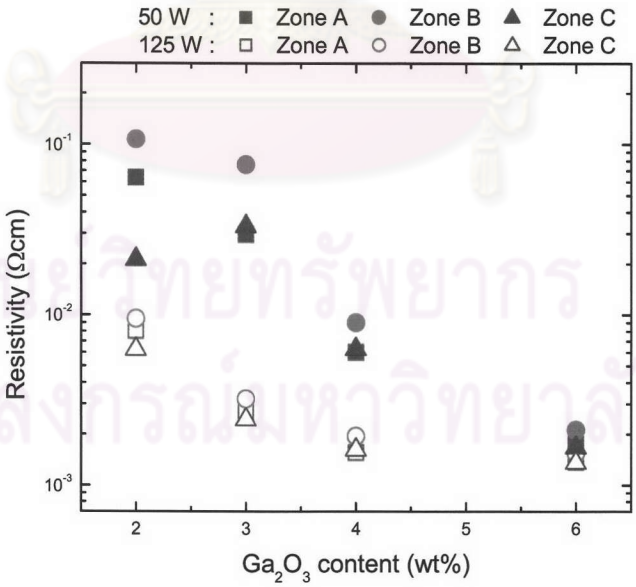

Figure 5.9: Resistivity of each zone of the GZO films prepared at different RF power and $P_{Ar} = 8.0 \times 10^{-3}$ mbar as a function of Ga_2O_3 content in the target

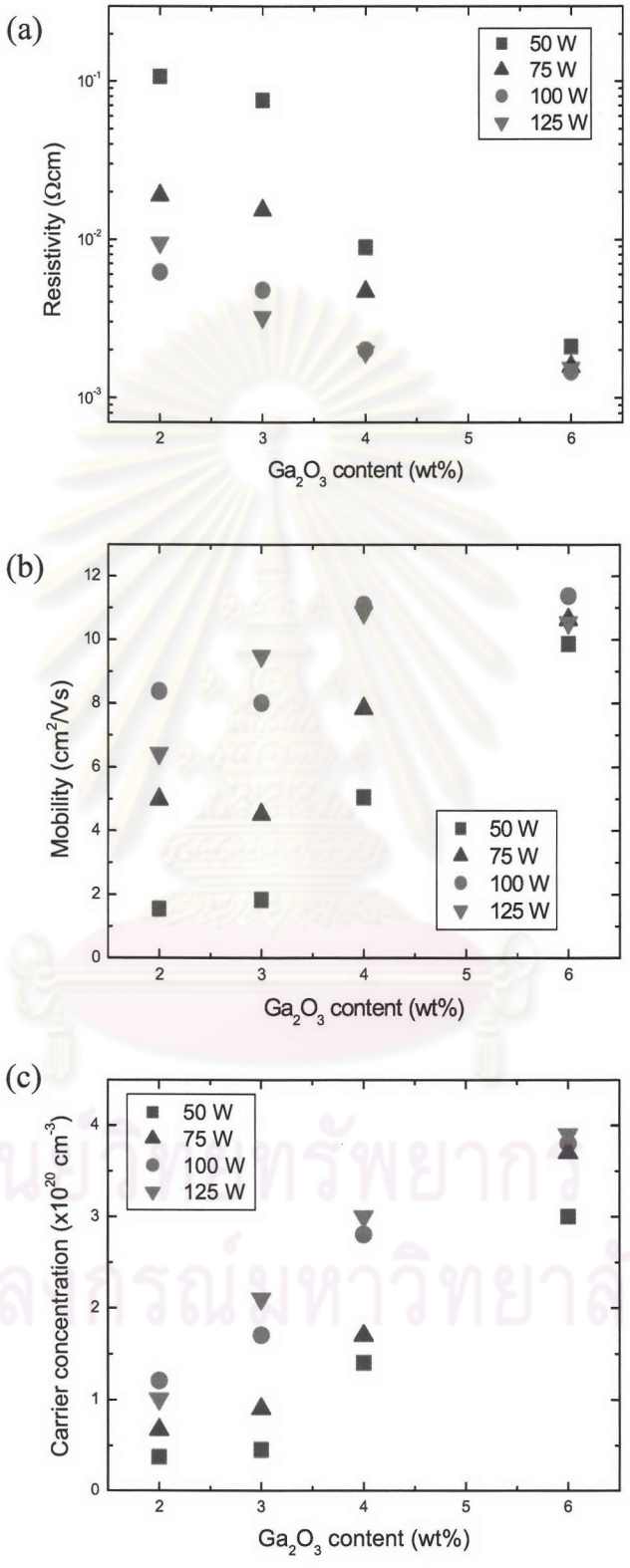

Figure 5.10: Dependence of resistivity (a), mobility (b) and carrier concentration (c) of GZO films on Ga_2O_3 content in the target. The films were deposited at the RF power of $50 - 125$ W and $P_{Ar} = 8.0 \times 10^{-3}$ mbar

increase while resistivity decreases with increasing Ga_2O_3 content for a given RF power. The results show the same trend as in Fig. 5.9. In the case of the films deposited using the RF power of 50 W, it can be clearly seen that the resistivity of the films decreases from 1.07×10^{-1} to 2.10×10^{-3} Ω·cm when the Ga_2O_3 content increases from 2wt% to 6wt%. Both carrier concentration and mobility increases from 3.70×10^{19} to 3.00×10^{20} cm^{-3} and from 1.55 to 9.86 cm^2/Vs, respectively.

In addition, for a given Ga_2O_3 content, the resistivity decreases with increasing RF power that is mentioned in the previous results. Figure 5.10(a) clearly shows that the resistivity widely differs for low Ga_2O_3 contents but very closely for high Ga_2O_3 contents. The lowest resistivity of 1.45×10^{-3} Ω·cm was obtained at the Ga_2O_3 content of 6wt% and the RF power of 100 W. Figure 5.10(b) and (c) show the highest mobility and carrier concentration of this sample, respectively. The result indicates that the decrease in resistivity is due to the increase of both mobility and carrier concentration.

The resistivity is proportional to the inverse of the product of the mobility and the carrier concentration. Therefore, the change in resistivity with RF power, especially in the case of low Ga_2O_3 content, is ascribed to the change in carrier concentration and/or mobility, which are characteristic parameters reflecting the stoichiometry and impurity contents of the film. This means that the donor defects, especially intrinsic donor, associated with oxygen vacancies or excess metal ions can be increased by increasing of RF power. Thus, the carrier concentration increases and the resistivity decreases due to non-stoichiometric of the films that corresponds to the structural properties as shown in Figs. 5.4 and 5.5. With increasing Ga_2O_3 content, the resistivity decreases, followed by the increasing of carrier concentration and mobility. Especially, the carrier concentration increases due to the contribution from Ga ions (extrinsic donor) on substitutional sites of Zn ions and Ga interstitial atoms, as well as from oxygen vacancies and Zn interstitial atoms (intrinsic donor).

For the most of films fabricated in this work, a high carrier concentration was obtained ($> 10^{20}$ cm^{-3}). The potential barriers associated to grain boundaries, which are the scattering centers of electron transport in the films, are proposed to

account for this effect. Both intrinsic and extrinsic donor increase the impurity density, but they also diminish the potential barriers between the grain boundaries [38]. The barriers can be so narrow such that the electrons are able to tunnel though the barriers. This means that the grain boundaries no longer limit the carrier scattering [14]. The importance of scattering mechanism is dependent on film quality and the carrier concentration [38, 39]. Therefore, the decrease in resistivity of the films is due to the increase in the mobility and carrier concentration.

For more details, Fig. 5.11(a) shows the dependence of resistivity and mobility on the Ga_2O_3 content in the target. These GZO thin films were deposited using the RF power of 100 W under Ar pressure of 8.0×10^{-3}mbar. It shows that the resistivity decreases gradually as increasing Ga_2O_3 content from 2 wt% to 4 wt% and becomes saturated when Ga_2O_3 content reaches 6 wt%. The change of resistivity is related to the change of mobility. The mobility is also saturated as the Ga_2O_3 content is increased from 4 wt% to 6 wt%. This suggests that there is no necessary reason to increase Ga_2O_3 content to higher than 6wt%. The relationship between the mobility and the carrier concentration can be observed in Fig. 5.11(b). Figure 5.11(c) shows the dependence of the resistivity and the carrier concentration on the Ga_2O_3 content. The carrier concentration increases because of higher Ga doping in lattice sites of the film.

According to the previous results, the resistivity decreases with increasing RF power and Ga_2O_3 content. Although the RF power increases from 100 W to 125 W, the resistivity is still in the range of order $10^{-3}\Omega$·cm. We note that the RF power of 125 W was at the boundary of our sputtering system. During sputtering at the RF power of 125 W, the temperature of the system is rising high due to the aggressive bombardment on the target and over the ability of the cooling system. Figure 5.12(a) shows the dependence of the electrical resistivity versus the Ga_2O_3 content for various Ar pressure. The resistivity differs insignificantly and also decreases with increasing of Ga_2O_3 content at all Ar pressure similar to that shown in the previous results. It was followed by the increase of the mobility and the carrier concentration. The lowest resistivity of $1.14\times10^{-3}\Omega$·cm was achieved for Ga_2O_3 content of 6 wt%

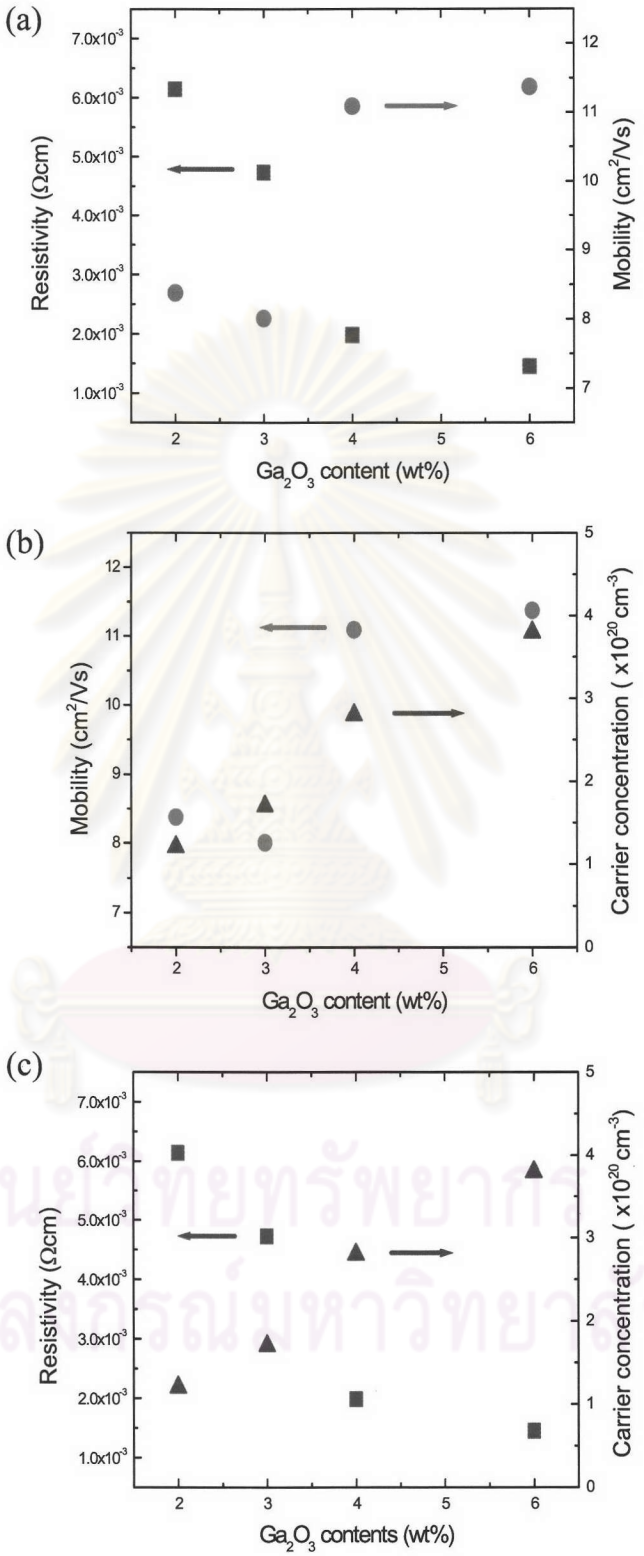

Figure 5.11: Dependence of electrical properties of GZO films prepared at the RF power of 100 W and $P_{Ar} = 8.0 \times 10^{-3}$ mbar on Ga_2O_3 content in the target

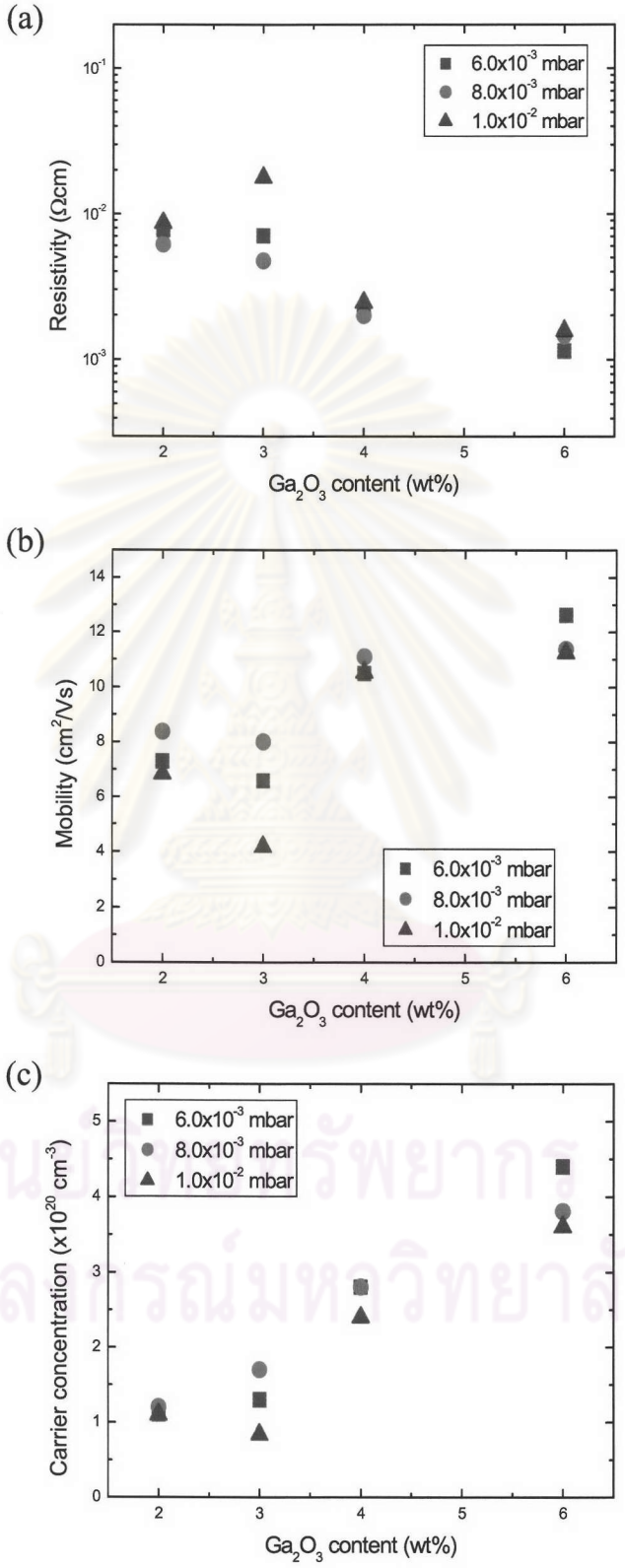

Figure 5.12: Dependence of resistivity (a), mobility (b) and carrier concentration (c) of GZO films on Ga_2O_3 content in the target. The films were deposited at different Ar pressure and the RF power of 100 W

GZO 4 wt%, RF 125 W	As-deposited	Annealing in the air
Resistivity, ρ (Ωcm)	1.93×10^{-3}	1.23
Mobility, μ (cm^2/Vs)	10.85	4.95
Carrier concentration, n (cm^{-3})	3.0×10^{20}	1.0×10^{18}

Table 5.1: The electrical properties of GZO 4 wt% thin film, prepared at the RF power of 125 W and 8.0×10^{-3} mbar, before and after annealing in air atmosphere at 400°C for 2 hrs

at Ar pressure of 6.0×10^{-3} mbar and the RF power of 100 W, whose corresponding mobility is 12.63 cm^2/Vs and carrier concentration is 4.36×10^{20} cm^{-3}, as shown in Figs. 5.12(b) and (c), respectively.

For a comparison of the effect of annealing, the electrical properties of GZO 4 wt% thin film before and after annealing in air atmosphere at 400°C for 2 hrs are shown in Table 5.1. It is observed that the resistivity of as-deposited GZO film was $1.93 \times 10^{-3} \Omega \cdot$cm, while the resistivity of the film increases substantially by three orders of magnitude after annealing. It is due to the decrease in the mobility and the carrier concentration. This suggests that annealing in the air could enhance the chemisorption of N_2 or O_2, and the formation of GaO_x or GaN_x reducing the density of the donor defects and the carrier concentration [32]. This formation can also reduces the Ga ions on substitutional sites and Ga interstitial atoms leading to the lower carrier concentration. GaO_x or GaN_x will lead to an increase in scattering centers and result in a decrease in mobility. In addition, more defects are annealed out, and the decrease of oxygen vacancies result in the high resistivity of the film [32]. Therefore, the electrical properties of GZO thin film can not be improved by annealing in air atmosphere.

5.4 Optical Properties

As for a representative, samples from zone B are used for the optical transmission measurement. Figure 5.13 shows the optical transmission (%T) of samples with different Ga_2O_3 content in the GZO target at the Ar pressure of 8.0×10^{-3} mbar and the RF power of 50, 100 and 125 W. The transmission spectra were measured at the wavelength in the range from 300 to 1500 nm. All samples, which were compared together, have a smooth surface and at about the same thickness. Their measured transmission spectra show interference fringes. The transmission of all films decreases with increasing RF power for a given Ga_2O_3 content. This suggests that the RF power is also one parameter on the optical transmission.

When the wavelength is below 1000 nm, the effect of the RF power on the transmission is small. However, there are slight decreases in transmission which depend on the RF power. Considering the difference of XRD patterns with the RF power in Figs. 5.4 and 5.5, this slight decrease in transmission may be attributed to the crystallinity of the films.

For a given Ga_2O_3 content, the crystallinity and transmission decrease with increasing RF power. Especially, it can be clearly seen at the wavelength above 1000 nm, the RF power strongly influences the transmission. A low RF power (50 W) maintains high optical transmission due to a perfect ZnO structure of the films, while a high RF power (125 W) reduces the transmission. This reduction of transmission with increasing RF power corresponds to the increasing carrier concentration in Fig. 5.10(c) quite well and can be explained by a free-carrier absorption.

The GZO thin films are poor crystallinity at high RF power. Then, the number of free electrons increase due to more donor defects. The increase of carrier concentration is attributed to high free-carrier absorption at long wavelength. Therefore, the optical transmission at infrared (IR) region decreases with increasing RF power.

The transmission spectra show more interference fringes as the growing of

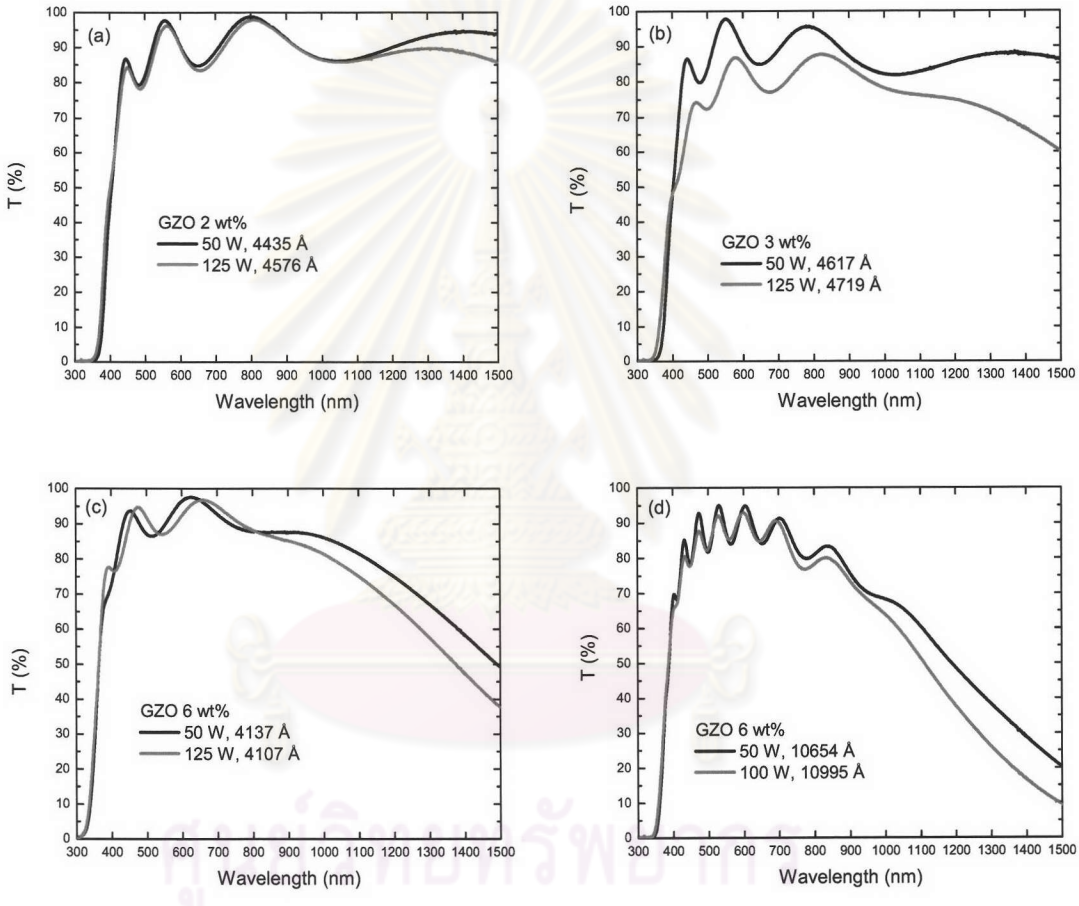

Figure 5.13: The optical transmission of GZO films prepared using the target with various Ga_2O_3 contents at different RF power and $P_{Ar} = 8.0 \times 10^{-3}$ mbar

the film thickness, as shown in Fig. 5.13(c), (d), and clearly in Fig. 5.14. For the increasing of the thickness of the GZO 6wt% thin films deposited by using the RF power of 100 W and the Ar pressure of 8.0×10^{-3} mbar. With increasing thickness, the transmission of the films is decreased due to the thickness effect leading to a decrease in light scattering losses [1].

Figure 5.15 shows the transmission spectra of the GZO thin films prepared from different targets by using the same sputtering condition. It is shown that the Ga_2O_3 content has a very strong impact on the transmission at long wavelengths. With increasing Ga_2O_3 content, the transmission decreases because of the increase of the carrier concentration. More Ga atoms can be substituted in the lattice sites, resulting in the increasing of the free-carrier absorption at the IR wavelengths.

The absorption edge is also shown to shift to shorter wavelengths as the increasing of Ga_2O_3 content. This effect is called blue-shift of the absorption edge. It is mainly attributed to the Burstein-Moss effect [1, 22], since the absorption edge of degenerate semiconductor is shifted to a shorter wavelengths region with increasing carrier concentration. Because the GZO thin film has a direct band gap as well as the pure polycrystalline ZnO, the optical energy gap (E_g) of the film can be obtained by plotting $(\alpha h\nu)^2$ vs. $h\nu$, where α is the optical absorption coefficient and $h\nu$ is the photon energy as shown in Fig. 5.16. The absorption edge for the direct interband transition is given by [32]

$$(\alpha h\upsilon)^2 = A(h\upsilon - E_g), \tag{5.3}$$

where A is a constant. The optical band gap can then be obtained from the interception of $(\alpha h\nu)^2$ versus $h\nu$ for direct allowed transition. The E_g value is determined by the extrapolation method of which the linear segments of the curves toward the x-axis gave the E_g values in the range $3.39 - 3.63$ eV for the films deposited at the RF power of 100 W and the Ar pressure of 8.0×10^{-3} mbar.

The variation of optical band gap as a function of Ga_2O_3 content is shown in Fig. 5.16. It shows that the band gap is widened (blue shift) with increasing Ga_2O_3 content. Since the energy gap of pure ZnO film is about 3.30 eV [22], it is evident

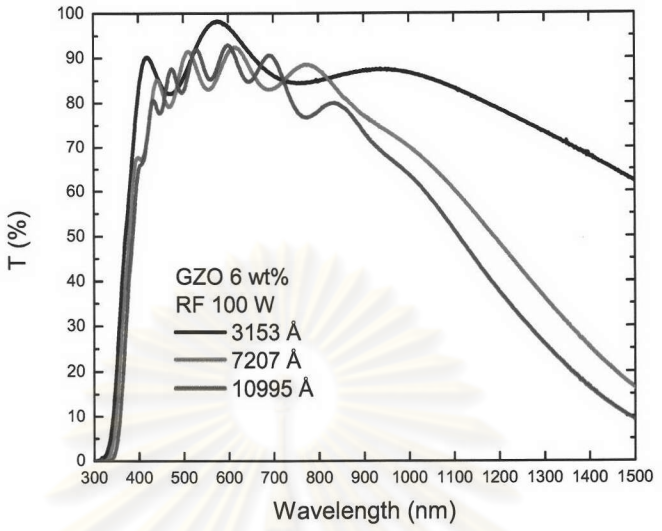

Figure 5.14: The optical transmission of GZO films at different thicknesses prepared using the target with Ga_2O_3 content of 6 wt%, the RF power of 100 W and $P_{Ar} = 8.0 \times 10^{-3}$ mbar

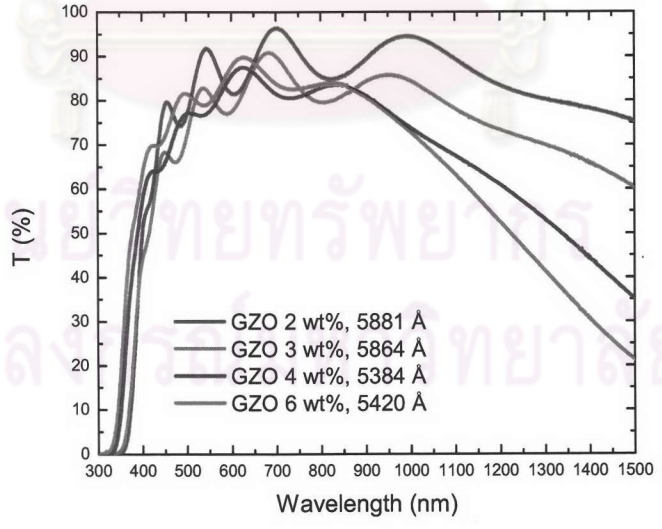

Figure 5.15: The optical transmission of different Ga_2O_3 contents in GZO films deposited at the RF power of 100 W and $P_{Ar} = 8.0 \times 10^{-3}$ mbar

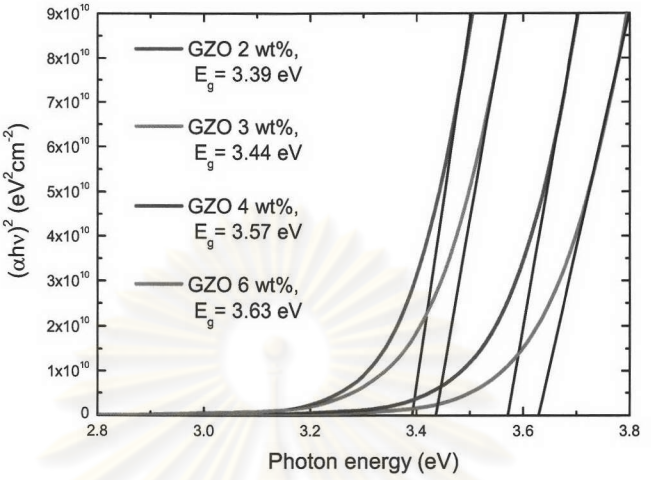

Figure 5.16: Plots of $(\alpha h\upsilon)^2$ vs. $h\nu$ for GZO thin films prepared at the RF power of 100 W and Ar pressure of 8.0×10^{-3} mbar

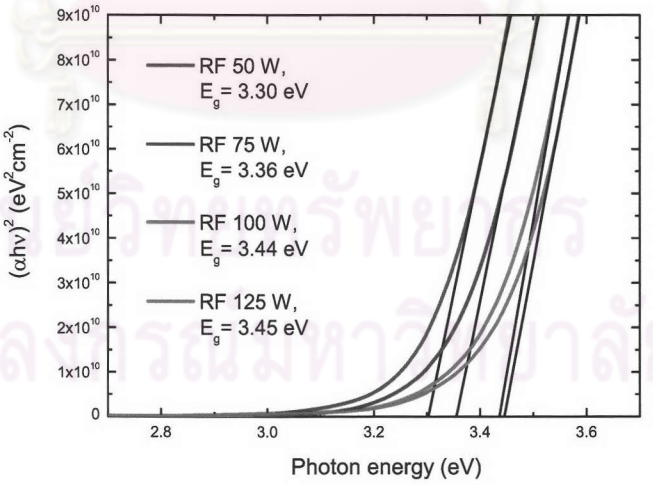

Figure 5.17: Plots of $(\alpha h\upsilon)^2$ vs. $h\nu$ for GZO thin films prepared using the target with Ga_2O_3 content of 3 wt% at Ar pressure of 8.0×10^{-3} mbar

that the change of optical band gap has been interpreted as a Burstein-Moss shift, where the change is the result of the shift of Fermi level in to the conduction band of degenerate semiconductors, as a result of increasing free-electron concentration. The Ga doping is responsible for this effect.

With the increase of Ga doping in ZnO film, the free-electron concentrations increase and the electrons occupy more conduction band states. When there is an interaction between photon and electron, the electron in valence band must have energy higher than the energy level of occupied state in the conduction band to cross from the filled valence band level to the unoccupied conduction band states.

In addition, for a given Ga_2O_3 content, the energy gap increases slightly when the RF power increases from 50 to 125 W. Figure 5.17 shows the plots of $(\alpha h\nu)^2$ versus $h\nu$ for GZO thin films prepared by the target with 3 wt% Ga_2O_3 at Ar pressure of 8.0×10^{-3} mbar and the RF power in the $50-125$ W range. The energy gaps are in the range $3.30-3.45$ eV. Furthermore, at the same range of the RF power, the energy gaps of the films deposited using the targets with Ga_2O_3 content of 2, 4 and 6 wt% are in the range $3.28-3.44$ eV, $3.42-3.57$ eV and $3.60-3.65$ eV, respectively. The lowest and highest energy gap values correspond to the highest and lowest resistivity of the films in Fig. 5.10, respectively.

According to the results in Figs. 5.16 and 5.17, it shows that the energy gap widens slightly as increasing RF power compared to increasing Ga_2O_3 content. When the RF power increases, the GZO thin films have more donor defects increasing the carrier concentration. However, the increase of Ga_2O_3 content has more influence to the increase of the energy gap. Therefore, the range of energy gap is widened with increasing Ga_2O_3 content due to increasing of high carrier concentration attributed to the Ga doping.